Doddrell, D., Glushko, V., & Allerhand, A. (1972) *J. Chem. Phys. 56*, 3683–3689.
Gerken, T. A. (1986) *Arch. Biochem. Biophys. 247*, 239–253.
Gerken, T., & Dearborn, D. (1984) *Biochemistry 23*, 1485–1497.
Gottschalk, A., & Bhargava, A. (1972) in *Glycoproteins: Their Composition, Structure, and Function* (Gottschalk, A., Ed.) Elsevier, New York.
Goux, W. J., Perry, C., & James, T. L. (1982) *J. Biol. Chem. 257*, 1829–1835.
IUPAC–IUB Joint Commission of Biochemical Nomenclature (1970) *Biochemistry 9*, 3471–3479.
Jardetzky, O., & Roberts, G. (1981) *NMR in Molecular Biology*, Academic, New York.
Jentoft, N. (1985) *Anal. Biochem. 148*, 424–433.
Kochetkoy, N., Chizhov, O., & Shashkov, A. (1984) *Carbohydr. Res. 133*, 173–185.
Kowalewski, J., Levy, G., Johnson, F., & Palmer, L. (1977) *J. Magn. Reson. 26*, 533–536.
Lemieux, R., Bock, K., Delbaere, L., Koto, S., & Rao, V. (1980) *Can. J. Chem. 58*, 631–653.
Opella, S., Nelson, D., & Jardetzky, O. (1976) *ACS Symp. Ser. No. 34*, 397–417.
Pavia, A., & Ferrari, B. (1983) *Int. J. Pept. Protein Res. 22*, 539–548.
Pfeffer, P., Parrish, F., & Unruh, J. (1980) *Carbohydr. Res. 84*, 13–23.
Prohaska, R., Koerner, T., Armitage, I., & Furthmayr, H. (1981) *J. Biol. Chem. 265*, 5781–5791.
Rao, B., Dua, V., & Bush, C. A. (1985) *Biopolymers 24*, 2207–2229.
Rosevear, P., Neunez, H., & Barker, R. (1982) *Biochemistry 21*, 1421–1431.
Sabesan, S., & Paulson, J. (1986) *J. Am. Chem. Soc. 108*, 2068–2080.
Schacter, H., & Williams, D. (1982) *Adv. Exp. Med. Biol. 144*, 3–28.
Shogren, R., Jamieson, A., Blackwell, J., & Jentoft, N. (1984) *J. Biol. Chem. 269*, 14657–14662.
Shogren, R., Jamieson, A., Blackwell, J., & Jentoft, N. (1986) *Biopolymers 25*, 1505–1517.
Shogren, R., Gerken, T. A., Jentoft, N., Jamieson, A., & Blackwell, J. (1987a) *Biophys. J. 51*, 84a.
Shogren, R., Jentoft, N., Gerken, T., Jamieson, A., & Blackwell, J. (1987b) *Carbohydr. Res. 106*, 317–327.
Van Halbeek, H., Dorland, L., Haverkamp, J., Veldink, G., Vliegenthart, F., Fournet, B., Ricart, G., Montreuil, J., Gathmann, W., & Aminoff, D. (1981) *Eur. J. Biochem. 118*, 487–495.

Oxygen Infrared Spectra of Oxyhemoglobins and Oxymyoglobins. Evidence of Two Major Liganded O_2 Structures†

William T. Potter,‡ Melvin P. Tucker,§ Robert A. Houtchens,‖ and Winslow S. Caughey*
Department of Biochemistry, Colorado State University, Fort Collins, Colorado 80523
Received January 15, 1987; Revised Manuscript Received March 19, 1987

ABSTRACT: The dioxygen stretch bands in infrared spectra for solutions of oxy species of human hemoglobin A and its separated subunits, human mutant hemoglobin Zurich (β63His to Arg), rabbit hemoglobin, lamprey hemoglobin, sperm whale myoglobin, bovine myoglobin, and a sea worm chlorocruorin are examined. Each protein exhibits multiple isotope-sensitive bands between 1160 and 1060 cm^{-1} for liganded $^{16}O_2$, $^{17}O_2$, and $^{18}O_2$. The O–O stretch bands for each of the mammalian myoglobins and hemoglobins are similar, with frequencies that differ between proteins by only 3–5 cm^{-1}. The spectra for the lamprey and sea worm hemoglobins exhibit greater diversity. For all proteins an O–O stretch band expected to occur near 1125 cm^{-1} for $^{16}O_2$ and $^{17}O_2$, but not $^{18}O_2$, appears split by ~25 cm^{-1} due to an unidentified perturbation. The spectrum for each dioxygen isotope, if unperturbed, would contain two strong bands for the mammalian myoglobins (1150 and 1120 cm^{-1}) and hemoglobins (1155 and 1125 cm^{-1}). Two strong bands separated by ~30 cm^{-1} for each oxy heme protein subunit indicate that two major protein conformations (structures) that differ substantially in O_2 bonding are present. The two dioxygen structures can result from a combination of dynamic distal and proximal effects upon the O_2 ligand bound in a bent-end-on stereochemistry.

Binding O_2 reversibly enables hemoglobins and myoglobins to function in O_2 delivery to widespread sites of oxygen utilization (Antonini & Brunori, 1971; Bunn & Forget, 1986). These heme proteins also contribute to oxidant stress by serving as electron donors to O_2 to produce oxy radicals and hydrogen peroxide [e.g., see Wallace et al. (1982), Kawanishi and Caughey (1985), Caughey and Watkins (1985), and Winterbourn (1985)]. The present understanding of how globin structures control O_2 transport and minimize O_2 reduction remains far from complete. The key question of how O_2 binds at heme sites has not been fully answered. The discovery of an oxygen isotope sensitive O–O stretch band near 1100 cm^{-1} in the infrared spectra for solutions of human oxyhemoglobin A and of bovine oxymyoglobin provided the first direct experimental evidence on bond type (i.e., an O–O bond order of 1.5) and a stereochemistry that is "bent end on" (Caughey et al., 1975). This stereochemistry is supported by X-ray and

† This research was supported by U.S. Public Health Service Grant HL-15980.
‡ Present address: Department of Laboratory Medicine and Pathology, University of Minnesota, Minneapolis, MN 55455.
§ Present address: SERI, Golden, CO 80401.
‖ Present address: Bioproducts—Central Research, Dow Chemical USA, Midland, MI 48640.

0006-2960/87/0426-4699$01.50/0

neutron diffraction crystallographic studies (Phillips, 1980; Phillips & Schoenborn, 1981; Shaanan, 1982, 1983; Brozozowski et al., 1984). However, it is now clear, as discussed below, that several O–O stretch bands are present in infrared spectra for oxyhemoglobins and oxymyoglobins in solution. Multiple O–O bands suggest multiple structures for liganded dioxygen.

Ligand vibrational spectra provide unique insight into the nature of ligand binding in heme proteins (Caughey, 1980; Yu, 1986). Ligand vibrational bands are not only sensitive to differences in the Fe–ligand bond but also to steric and electrostatic interactions experienced by the ligand in the heme pocket. Infrared stretch bands have been observed for CO, CN^-, NO, and N_3^- liganded to a variety of hemoglobins and myoglobins. Discrete, multiple stretch bands are observed to vary with changes in temperature, pH, and solvent conditions (McCoy & Caughey, 1970; Maxwell & Caughey, 1976; Choc & Caughey, 1981; Caughey et al., 1981; Shimada & Caughey, 1982; Caughey et al., 1983; Yoshikawa et al., 1985). The presence of multiple bands is consistent with the occurrence of several rapidly interconverting conformers (structures) at a single heme site. Carrying out similar studies with the O_2 ligand has been limited by the greater experimental difficulty in obtaining accurate spectra. The O–O stretch bands occur in a region of the infrared spectrum where strong absorbance by water, protein, and porphyrin also occurs (Caughey, 1980). Furthermore, the tendency of oxy species to autoxidize makes them less stable than the carbonyl, cyano, or azido species.

In the pioneering infrared studies only a single O–O stretch band at 1107 cm^{-1} for $HbA^{16}O_2$[1] and 1103 cm^{-1} for bovine $Mb^{16}O_2$ could be established unequivocally (Barlow et al., 1973; Maxwell et al., 1974). In brief reports additional bands near 1150–1160 (Alben et al., 1978; Caughey et al., 1979) and 1130 cm^{-1} (Caughey et al., 1979, 1982) were convincingly demonstrated by use of more sensitive infrared methods. However, the structural basis for multiple O–O bands remains unclear. This paper reports an extension of the earlier studies to include O–O stretch bands for several well-studied hemoglobins and myoglobins with diversity in structure and O_2 binding characteristics. Each protein exhibits multiple $^{16}O_2$, $^{17}O_2$, and $^{18}O_2$ stretch bands which are interpreted as due to two major structures (conformers) for the adduct formed from O_2 and heme. The nature and possible origins of the structural differences for the two conformers are considered.

Materials and Methods

Preparation of Proteins. All procedures were carried out at 4 °C. Bovine oxymyoglobin was isolated directly from fresh beef hearts by a modification of a common method (Yamazaki et al., 1964) in which a molecular sieve column was used (Gotoh & Shikama, 1974). Sperm whale metMb was purified from salt-free lyophilized powder (Sigma) and reduced under anaerobic conditions directly with excess dithionite (Virginia Chemical) with anaerobic removal of any byproducts (Rothgeb & Gurd, 1978; Jelkman & Bauer, 1976). Deuterium-exchanged sperm whale metMb was prepared by four dilution/reconcentration cycles of a 15-fold volume excess of D_2O (99.8 atom %; Sigma) over 72 h and reduced as described above. Human HbO_2 was obtained from fresh human blood by standard methods (Riggs, 1981). Separated subunits of human HbACO were prepared by the method of Bucci (1981) as modified by Yip et al. (1977). O_2 substitution was performed by flushing the separated subunits with moist O_2 while rotating the sample under strong tungsten lights. The oxygenated subunits were used within 24 h of preparation and contained less than 10% met species by visible spectroscopy. HbZhCO was isolated by the method of Huisman (Dozy et al., 1986) from an individual heterozygous for HbZh and used immediately following oxygenation as described for the separated subunits. Less than 3% HbZhCO was detected in oxygenated HbZh samples by visible or infrared spectroscopy. Rabbit (*Oryctolagus cuniculus*) red cells were obtained by cardiac puncture, and the plasma and buffy coats were removed by centrifugation. The red cells were washed 3 times with 1% NaCl and either used directly or lysed hypotonically and observed following removal of the cellular debris by centrifugation at 30000*g* for 60 min. Lamprey (*Petromyzon marinus*) blood was obtained from adult animals by direct ventricular incision with isotonic sodium citrate as an anticoagulant. Lamprey HbO_2 hemolysates were prepared and deionized as described for human HbA. Ion-exchange chromatography on diethylaminoethyl-Sephadex A-50 equilibrated with 2.5 mM Tris (pH 8.5) showed multiple bands. The major band (~35% of the total) eluted at 5 mM Tris (pH 8.5) and was shown by HPLC to have a molecular weight of approximately 20600 (Himmel & Squire, 1981a). Only this fraction was used for these studies. The high molecular weight chlorocruorin of sea worm (*Botamilla leptochaeta*) was isolated by the method of Orii and Washio (1977) by Dr. S. Yoshikawa. Only freshly isolated, unfrozen chlorocruorin with a molecular weight of 2.9×10^6 as observed by sedimentation velocity analysis and HPLC (Himmel & Squire, 1981b) was used.

Recording of Spectra. Infrared spectra were measured on a Perkin-Elmer Model 180 spectrophotometer interfaced with a Tektronix 4051 computer. Multiple spectra (8–25) were recorded with 2.8-cm^{-1} resolution at 1100 cm^{-1} and averaged to increase signal to noise levels. Matched, constant temperature cells with CaF_2 (3-mm) windows were used for all spectra. O_2 isotope substitution was accomplished by at least three exchanges on rotating samples with excess $^{17}O_2$ (90.6 atom %; Miles) or $^{18}O_2$ (99.7 atom %; Prochem) over a 4-hour period. Difference spectra were obtained by subtraction of the computer-stored averaged spectra of equivalent, isotopically substituted samples. Visible spectra of samples with CaF_2 windows were recorded directly within the intact infrared cell on a Cary 17 spectrophotometer. Sample stability was confirmed before and after all infrared spectra reported here. Further details of spectral methods for the measurements are described in previous papers (Maxwell & Caughey, 1978; Caughey, 1980).

Results

Measurement of O–O Stretch Bands. The infrared spectrum for a solution of human adult hemoglobin A with liganded $^{16}O_2$ over the range from 1300 to 1000 cm^{-1} is shown in Figure 1 (top trace). The solution contains 20 mM heme in 20 mM Tris buffer, pH 7.5 at 4 °C. The sample cell and reference cell (with water) have comparable path lengths, ca. 0.055 mm. The trace shown represents an average of 12 single scans. Offset below the $HbA^{16}O_2$ spectrum is an analogous spectrum for $HbA^{18}O_2$. The difference spectrum ($^{16}O_2 - {}^{18}O_2$) reveals dioxygen isotope sensitive bands due to the coordinated O_2. These bands, positive bands for $^{16}O_2$ and negative bands for $^{18}O_2$, are seen more clearly in the expanded difference spectrum of the lower panel in Figure 1. The strong absor-

[1] Abbreviations: HbA, human hemoglobin A; HbACO, (carbonmonoxy)hemoglobin A; $HbAO_2$, oxyhemoglobin A; HbO_2, oxyhemoglobin; HbZh, human mutant hemoglobin Zurich; Mb, myoglobin; Tris, tris(hydroxymethyl)aminomethane; HPLC, high-performance liquid chromatography.

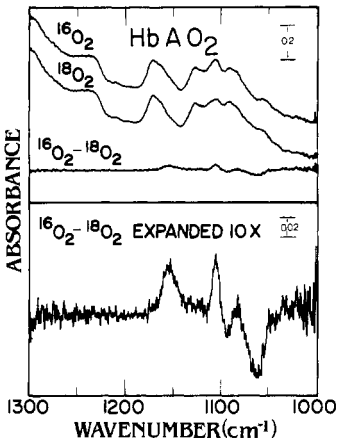

FIGURE 1: Infrared spectra of human hemoglobin A liganded with $^{16}O_2$ and $^{18}O_2$ in the 1300–1000-cm^{-1} region. (Upper) Spectra observed for solutions of 20 mM $HbAO_2$ in 20 mM Tris buffer, pH 7.5 at 4 °C, with water in the reference cell. Each spectrum represents an average of 12 scans using cells with 3-mm CaF_2 windows and path lengths of 0.055 mm. The $^{18}O_2$ spectrum is offset below the $^{16}O_2$ spectrum. The $^{16}O_2 - {}^{18}O_2$ difference spectrum is shown on the base line. (Lower) The $^{16}O_2 - {}^{18}O_2$ difference spectrum expanded 10-fold.

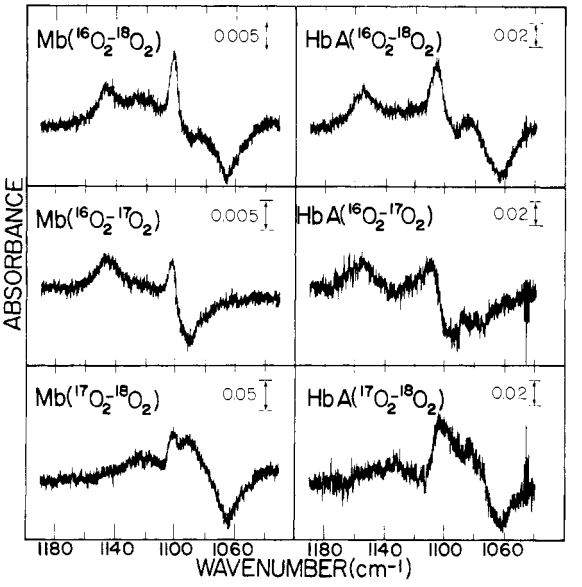

FIGURE 2: Oxygen isotope infrared difference spectra for sperm whale oxymyoglobin and human oxyhemoglobin A in the 1190–1030-cm^{-1} region. Conditions: 11 mM MbO_2 in 30 mM Tris buffer, pH 8.5, 1 °C; 20 mM HbO_2 in 20 mM Tris buffer, pH 7.5, 4 °C.

bance in the 1300–1000-cm^{-1} region by water, protein, heme, and buffer makes the use of difference spectra between dioxygen isotopes essential for the identification of the low-intensity O–O stretch bands. The solutions and cells from which the difference spectra are obtained must be carefully matched. Slight changes in path length, temperature, heme protein concentration, or extent of O_2 saturation can result in artifactual bands. Partial autoxidation and associated protein precipitation must be avoided. Thin films of denatured protein on the cell windows can result in an intense band near 1045 cm^{-1}. Autoxidation rates for oxy-Hbs and oxy-Mbs are highly sensitive to pH (Caughey et al., 1979; Wallace et al., 1982). With the proteins studied here, the use of a pH range from 7.5 to 8.5 minimizes autoxidation. The choice of buffer is also important since autoxidation rates are somewhat buffer dependent and buffer molecules may absorb strongly in the O–O stretch band region. Phosphate, [bis(2-hydroxyethyl)-amino]tris(hydroxymethyl)methane, 2-(*N*-morpholino)-ethanesulfonic acid, and 3-(*N*-morpholino)propanesulfonic acid are each strongly absorbing in the O–O stretch region and can easily mask the relatively weak O–O bands if used at high concentrations.

Oxygen isotope difference spectra of acceptable quality can be recorded directly with a dual-beam infrared spectrophotometer only if the sample and reference cells are very precisely matched. The required precision in matching can be extremely difficult to achieve with commercially available cell windows. The need for such matching can be avoided by the use of the same sample cell for both $^{16}O_2$ and $^{18}O_2$ solutions. Difference spectra are then obtained by subtraction of computer-stored spectra recorded against only an approximately matched reference cell that contains water or buffer. The use of water (or buffer) in the reference cell enhances detector sensitivity, which depends upon the ratio of sample absorbance to reference absorbance in the dual-beam dispersive instrument used in this study.

The detection of O–O stretch bands depends critically on the choice of the reference hemoglobin solution. Difference spectra between $^{16}O_2$, $^{17}O_2$, and $^{18}O_2$ species of sperm whale myoglobin and of human HbA are shown in Figure 2. For both proteins the determination of all the O–O bands associated with each isotope requires the comparison of the three types of difference spectra: $^{16}O_2 - {}^{18}O_2$, $^{16}O_2 - {}^{17}O_2$, and $^{17}O_2 - {}^{18}O_2$. Analysis reveals that each difference spectrum has a central region where overlapping oxygen isotope sensitive bands are present. The shape of the 1100-cm^{-1} region in the $^{16}O_2 - {}^{18}O_2$ spectrum indicates slight overlap of $^{16}O_2$ and $^{18}O_2$ bands. The $^{16}O_2 - {}^{17}O_2$ spectrum shows even greater overlap in this region, and only the highest frequency band for $^{16}O_2$ near 1150 cm^{-1} experiences no overlap from an $^{17}O_2$ band. In the $^{17}O_2 - {}^{18}O_2$ spectrum, only the lowest frequency band for $^{18}O_2$ is not overlapped by $^{17}O_2$ bands. $^{16}O_2$ bands are found in three regions: a moderately broad region near 1155–1150 cm^{-1}, a wide, lower absorbance region centered near 1130 cm^{-1}, and a region near 1107–1103 cm^{-1} with a sharp, strong band. $^{18}O_2$ bands are found in two regions: a region near 1095–1090 cm^{-1} with a weak band and a region near 1065 cm^{-1} with a broad stronger band. Although $^{17}O_2$ bands are more obscured by overlap than are the $^{16}O_2$ or the $^{18}O_2$ bands and the presence (<20%) of mixed isotopes is possible, the comparison of the three types of difference spectra indicates that $^{17}O_2$ bands occur in three regions: one near 1130 cm^{-1} with a weak band, another near 1103 cm^{-1} with a sharper, strong band, and another near 1095 cm^{-1}, with a possible shoulder at lower frequency.

Other types of difference spectra were also investigated to further clarify the positions of the O–O stretching bands, especially near 1100 cm^{-1}. Figure 3 shows the difference spectra for O_2 – CO or $O_2 - {}^{15}NO$. For HbO_2, major $^{16}O_2$ bands are seen at 1155 and 1106 cm^{-1}, locations also detected in $^{16}O_2 - {}^{18}O_2$ difference spectra. However, compared with the $^{16}O_2 - {}^{18}O_2$ difference spectrum, there is less absorbance near 1120 cm^{-1} in the $^{16}O_2$ – CO spectrum. Furthermore, two small bands occur near 1090 cm^{-1} with a shape suggestive of a derivative-shaped absorbance change; although minor, this feature is consistently observed. $^{18}O_2$ bands are observed near 1095 and 1065 cm^{-1} with either CO or ^{15}NO reference species; the 1095-cm^{-1} band is more intense than that observed in $^{16}O_2 - {}^{18}O_2$ spectra. The derivative-shaped absorbance difference near 1090 cm^{-1} is also present in the $^{18}O_2$ – CO spectrum although it is not as well defined as in the $^{16}O_2$ – CO spectrum. A weaker derivative-shaped absorbance change can also be detected in the same region for the oxy vs. nitrosyl spectra of Figure 3. Isotope substitution in either CO or NO has no

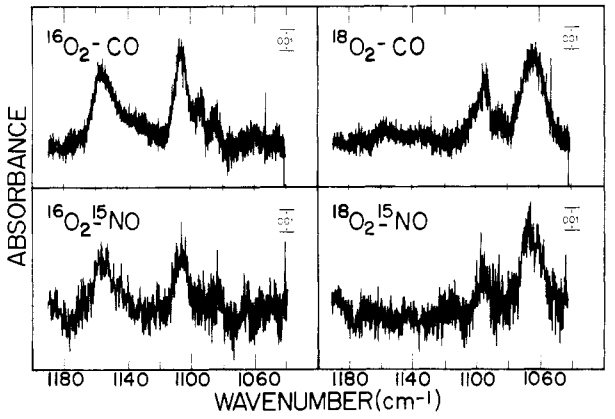

FIGURE 3: Difference infrared spectra for human hemoglobin A liganded to $^{16}O_2$, $^{18}O_2$, $^{12}C^{16}O$, or $^{15}N^{16}O$. Conditions: 15 mM Hb in 20 mM Tris buffer, pH 7.5, at 4 °C.

Table I: Infrared Dioxygen Stretch Band Parameters for Oxyhemoglobins and Oxymyoglobins[a]

heme protein	ν^b_{0-0} ($\Delta\nu_{1/2}$)[c] for $^{16}O_2$ (cm^{-1})			ν^b_{0-0} ($\Delta\nu_{1/2}$)[c] for $^{18}O_2$ (cm^{-1})	
HbA (red cells)	1155 (16)	[1132]	1106 (9)	1094 (7)	1065 (20)
HbA (stripped)	1155 (15)	[1130]	1106 (8)	1094 (6)	1065 (18)
HbA α-subunit	1152 (14)	[1127]	1106 (7)	1095 (9)	1065 (18)
HbA β-subunit	1155 (14)	[1138]	1108 (8)	1095 (9)	1065 (18)
HbZh	1156 (15) 1151 (15)	[1127]	1107 (10)	~1095	1066 (21)
rabbit Hb (red cells)	1155 (15) 1145 sh	[1125]	1107 (9)	1095 (9)	1065 (18)
sperm whale Mb	1148 (13)	[1125]	1103 (6)	1090 (9)	1065 (16)
bovine Mb	1151 (13)	[1127]	1104 (6)	1090	1065 (18)
lamprey Hb	1145 (15)	[1125]	1107 (11)		1063 (14)
chlorocruorin	[1165]	[1127]	1107 (11)		1071 (13)

[a] Band frequencies and bandwidths are measured from $^{16}O_2$ – $^{18}O_2$ difference spectra measured under the same conditions a those used in Figures 4 and 5. [b] Frequencies in brackets are broad bands of low intensity with no clear maximum. [c] Approximate half-bandwidths are shown in parentheses.

effect on the difference spectra. Differences in protein and/or heme infrared spectra between oxygenyl and carbonyl (or nitrosyl) species may result in this derivative-shaped feature near 1090 cm^{-1} in the difference spectra since this feature appears only in difference spectra for heme proteins with different Fe^{2+} ligands. In $^{16}O_2$ – deoxy and $^{16}O_2$ – met difference spectra (not shown) the O–O stretch bands could not be satisfactorily observed. The ensemble of infrared absorbance differences between the structurally distinct oxy and deoxy or met species is evidently extensive enough to mask the direct observation of the O–O stretch bands. Oxygen isotope difference spectra are expected to reflect the least interference from vibrations other than those for coordinated O_2. The $^{16}O_2$ – $^{18}O_2$ spectra do overlap near 1100 cm^{-1}, but they experience much less overlap than with $^{16}O_2$ – $^{17}O_2$ or $^{17}O_2$ – $^{18}O_2$ spectra. Nevertheless, O_2 – CO spectra are helpful in O–O band characterization (e.g., compare spectra in Figures 2 and 3), and the carbonyl species has the added advantage of unusually high stability.

Effects of Protein Structure on the Infrared O–O Stretching Vibrations. Figures 4 and 5 show the O_2 IR spectra obtained for Hbs and Mbs that vary widely in structure, in affinity for O_2, and in rates of O_2 binding and/or dissociation. The O–O stretch band parameters are listed in Table I.

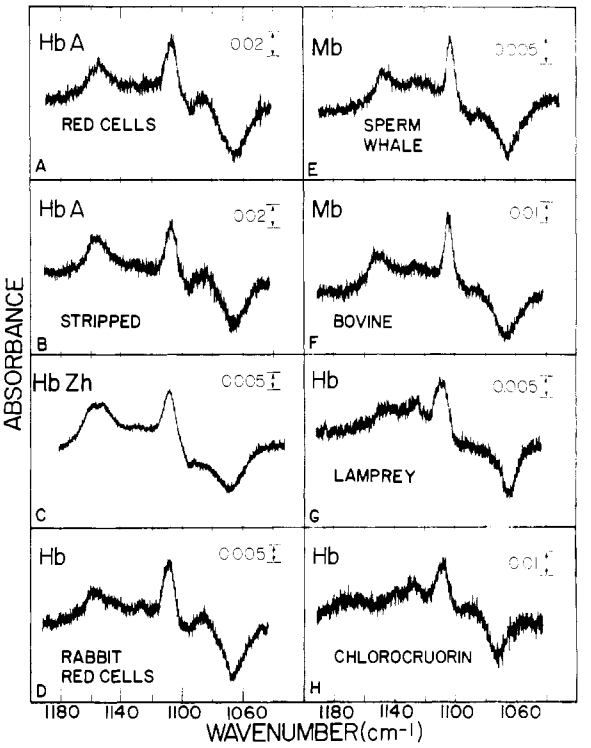

FIGURE 4: Infrared difference spectra for hemoglobins and myoglobins liganded with $^{16}O_2$ and $^{18}O_2$. Conditions: (A) washed human packed red cells, washed in isotonic saline at 4 °C; (B) purified human HbA in 10 mM K_3PO_4 buffer, 80 mM KCl, pH 7.0 at 4 °C; (C) HbZh in 10 mM Tris buffer, pH 8.0 at 4 °C; (D) packed rabbit red cells, washed in isotonic saline, 2 °C; (E) sperm whale Mb in 30 mM Tris buffer, pH 8.5 at 4 °C; (F) bovine heart Mb in 10 mM Tris buffer, pH 8.5 at 4 °C; (G) lamprey Hb in 5 mM Tris buffer, pH 8.5 at 1 °C; and (H) sea worm chlorocruorin in 10 mM K_3PO_4 buffer, pH 7.3 at 1 °C. The concentration for each heme protein was 5 mM or greater.

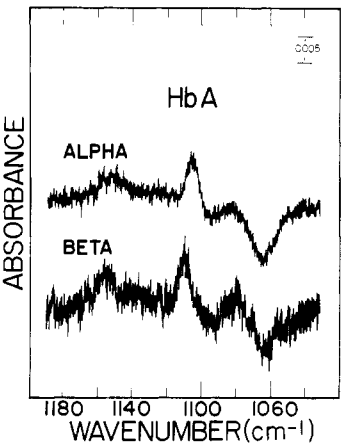

FIGURE 5: Oxygen isotope infrared difference spectra for separated α- and β-subunits of human $HbAO_2$. α-Subunits are in 40 mM Tris buffer, pH 8.2 at 4 °C. β-Subunits are in 10 mM K_3PO_4 buffer, pH 7.4 at 4 °C. Both subunits are ~6 mM in heme.

In Figure 4A,B the spectra for human $HbAO_2$ within the natural environment of packed red cells is compared to that observed for the purified protein stripped of organic phosphates. Within the available resolution and sensitivity, no significant differences were observed between red cells and isolated protein (Table I). As shown in Figure 5, the spectra of the isolated α- and β-subunits of HbA are similar, but $^{16}O_2$ bands for the α-subunits are observed at a 2–3 cm^{-1} lower frequency than the β-subunits. Therefore, the spectrum of the intact $\alpha_2\beta_2$ tetramer contains nearly equal contributions to each

O–O band from both types of subunit. Somewhat greater differences in spectra for α- and β-subunits are noted for hemoglobin Zurich O_2 ($HbZhO_2$), a mutant human hemoglobin in which the distal histidine of the β-subunits is replaced by arginine (Figure 4C). Two bands at 1156 and 1151 cm^{-1} are indicated in the $HbZh^{16}O_2$ spectrum, whereas a single band centered at 1155 cm^{-1} appears in the $HbA^{16}O_2$ spectrum. Rabbit Hb exhibits an $^{16}O_2$ spectrum with greater intensity at 1145 cm^{-1} (Figure 4D) than is found for the HbA spectrum.

The myoglobins from bovine and sperm whale (Figure 4E,F) exhibit spectra that differ only subtly from each other but are consistently shifted to lower frequencies compared to $HbAO_2$ spectra. The band comparable to the 1155-cm^{-1} band in $HbA^{16}O_2$ is found near 1150 cm^{-1} in the $Mb^{16}O_2$ spectra, and the 1106-cm^{-1} HbA band appears near 1103 cm^{-1} for the Mbs. The 1094-cm^{-1} $HbA^{18}O_2$ band appears at 1090 cm^{-1} in $Mb^{18}O_2$ spectra. The 1065-cm^{-1} band is observed at the same frequency for both types of spectra. Lamprey Hb, a single subunit monomeric protein, and chlorocruorin, a "giant Hb" with highly aggregated multiple subunits, both exhibit spectra with an intense $^{16}O_2$ band at 1107 cm^{-1}, as do the other Hbs, but differ markedly from all the other heme protein spectra in other respects (Figure 4G,H). All the spectra show absorbance for $^{16}O_2$ in the 1130–1120-cm^{-1} region. This region exhibits the greatest variability among the different hemoproteins, but the low band intensities hamper the determination of accurate band parameters. There is no $^{16}O_2$ band for chlorocruorin near 1155–1150 cm^{-1}, and the highest frequency $^{16}O_2$ band for lamprey is found at a much lower frequency than is observed for HbA (Table I). Absorbance in the 1130–1120-cm^{-1} region is especially clear in the chlorocruorin and lamprey spectra.

The $^{18}O_2$ band at 1095 cm^{-1} is difficult to establish in $^{16}O_2 - {}^{18}O_2$ spectra due to overlap of positive $^{16}O_2$ absorbance with negative $^{18}O_2$ absorbance. An $^{18}O_2$ band near 1095 cm^{-1} is evident in the $^{18}O_2$ – CO spectra (Figure 3), but the extent of interference due to the difference between O_2 and CO liganded species cannot be accurately determined. The $^{18}O_2$ band(s) near 1095 cm^{-1} is (are) clearly different for $HbZhO_2$ when compared with the $HbAO_2$ spectrum (Figure 4); however, splitting in this region of the $HbZh^{18}O_2$ spectrum into two bands is not observed. With lamprey Hb and chlorocruorin, the presence of an $^{18}O_2$ band near 1095 cm^{-1} is not evident. The spectra of lamprey and chlorocruorin also differ significantly from $HbA^{18}O_2$ in the band parameters of the 1065-cm^{-1} band (Figure 4 and Table I).

Effects of D_2O/H_2O Exchange on MbO_2 Spectra. Sperm whale myoglobin $^{16}O_2 - {}^{18}O_2$ difference spectra in D_2O and in H_2O show that replacement of H_2O by D_2O results in no large shifts in frequency for the major $^{16}O_2$ bands or the $^{18}O_2$ band at 1065 cm^{-1} (Figure 6). However, small differences in the two spectra can be detected. For example, in D_2O the $^{16}O_2$ absorbance near 1120 cm^{-1} is somewhat less intense and the $^{18}O_2$ band near 1090 cm^{-1} shifts 3–4 cm^{-1} to lower frequency compared to the spectrum in H_2O.

Discussion

Measurement of O–O Stretch Bands for Oxygen Bound to Heme Proteins. The infrared O–O stretch bands for oxygenyl ligands of heme proteins are more difficult to measure accurately than are bands for carbonyl, cyano, or azido ligands. The greater difficulty arises from several factors: (1) many absorbers other than coordinated dioxygen absorb strongly in the spectral region near 1100 cm^{-1}, (2) the oxy heme proteins are less stable, (3) multiple O–O bands of low intensity are exhibited, and (4) no species of heme protein yet found is

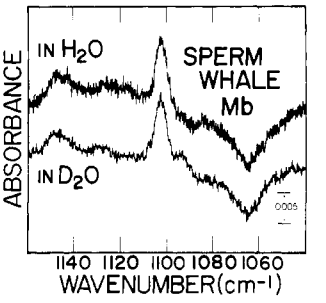

FIGURE 6: Dioxygen isotope ($^{16}O_2 - {}^{18}O_2$) infrared difference spectra for sperm whale MbO_2 in H_2O and in D_2O. Mb concentration is ~10 mM in 30 mM Tris buffer, pH 8.5, in H_2O and pD 8.65 in 30 mM deuteriated Tris buffer at 4 °C.

completely appropriate for use as a reference in order to record a difference spectrum that is solely due to O–O stretch bands. As shown in Figure 1, the contribution of O–O bands to the total absorbance is very small even at a high protein concentration (20 mM in heme). The strong absorbance by water limits the cell path lengths that will allow sufficient energy to pass through the cell. Reducing the path length requires an increase in the oxy heme protein concentration in order to maintain the same number of liganded O_2 vibrators in the light path. The signal to noise ratios can be improved slightly by the exchange of D_2O for H_2O (Figure 6) because D_2O absorbs less than H_2O at 1100 cm^{-1} (Caughey, 1980), but above 1150 cm^{-1} D_2O has a strong absorbance that can interfere with higher frequency O–O bands. Thus many factors can result in artifactual bands in difference spectra. Nevertheless, with suitable precautions to avoid such artifacts, authentic O–O stretch bands can be detected if sufficiently high protein concentrations are used.

Interpretation of Spectra. The O_2 ligand infrared spectra reported here are consistent with each type of protein subunit exhibiting three readily detected bands for $^{16}O_2$ and $^{17}O_2$ but only two bands for $^{18}O_2$. The heavy isotopes cause red shifts and alters the number, shapes, and intensities of the O–O stretch bands. Although red shifts are expected, the changes in the number and shapes of bands cannot be attributed to a change in the oxygen atom mass. For example, in CO infrared spectra for bovine myoglobin carbonyl, the four C–O stretch bands observed for the single protein subunit (Caughey et al., 1981; Shimada & Caughey, 1982) are reasonably assigned to four different protein structures (conformers). The band intensities reflect the relative stabilities of the respective heme carbonyl conformers. Substitution of ^{13}C and/or ^{18}O in the CO ligand causes predictable red shifts without altering the number, shapes, or intensities of the C–O bands. Thus the oxygen isotope effects observed in O–O stretch spectra are more complex than can be interpreted as one band per one protein structure. The unexpected complexity must result from vibrational coupling that perturbs the O–O vibrations differently for the three isotopes. Unfortunately, vibrational perturbations are not well understood. However, in general, perturbations may either shift the frequency or split a single band into several bands and do not decrease the number of bands (Bajdor et al., 1984; Kincaid et al., 1985).

Insight into the perturbations of the O–O stretch bands is gained from an examination of isotope effects. The spectra for the mammalian myoglobins and hemoglobins contain a highest frequency $^{16}O_2$ band near 1155–1150 cm^{-1} that appears shifted to near 1095–1090 cm^{-1} in spectra for $^{18}O_2$. The shift of 60 cm^{-1} is only about 5 cm^{-1} less than that predicted by reduced mass calculations. The predicted location for a $^{17}O_2$ band corresponding to either the band at 1155–1150 cm^{-1} for

$^{16}O_2$ and/or the band at 1095–1090 cm^{-1} for $^{18}O_2$, on the basis of reduced mass calculations, is at 1120–1115 cm^{-1}, or at 1125–1120 cm^{-1} if the isotope shift is 5 cm^{-1} less than the calculated value. However, the $^{17}O_2$ spectra lack bands in this region although they do exhibit a weak band at a slightly higher frequency (~1130 cm^{-1}) (Figure 2).

The lowest energy bands for each isotope also fail to differ in frequency to the extent expected on the basis of mass differences. Neither $^{17}O_2$ nor $^{18}O_2$ spectra contain a band that corresponds to the expected isotope shift from the strong lowest frequency $^{16}O_2$ band at 1107–1103 cm^{-1}. However, the lowest frequency band for $^{17}O_2$ at 1095–1090 cm^{-1} does correlate well in terms of expected isotope shift with the band near 1065 cm^{-1} for $^{18}O_2$. The locations of the lowest frequency bands for the $^{17}O_2$ and $^{18}O_2$ isotopes lead to a predicted $^{16}O_2$ band at 1125–1120 cm^{-1} (1130–1125 cm^{-1} represents a maximum calculated shift). Thus the analysis of expected isotope shifts supports the presence of a band in the region near 1125–1120 cm^{-1} for both $^{16}O_2$ and $^{17}O_2$. However, since the spectra observed for $^{16}O_2$ and $^{17}O_2$ (Figure 2) each show a strong sharp absorbance near 1105 cm^{-1} and a weak broader absorbance near 1130 cm^{-1} but no distinct band in the 1125–1120-cm^{-1} region as expected from the mass calculations discussed above, we conclude that two of the three observed bands for the $^{16}O_2$ and $^{17}O_2$ isotopes result from splitting of a vibration near 1125–1120 cm^{-1}.

The analysis of the observed O–O spectra in terms of a perturbing vibration near 1125–1120 cm^{-1} considered above is shown schematically in Figure 7. Spectra are shown in the top panel where each isotope exhibits distinctly different multiple bands. In the middle panel postulated unsplit O–O bands (crosshatched) at 1125–1120 cm^{-1} are superimposed on the $^{16}O_2$ and $^{17}O_2$ spectra. These crosshatched bands correspond to the lower frequency true $^{16}O_2$ vibration and the higher frequency true $^{17}O_2$ vibration. The proposed coupling of a perturbing vibration near 1125 cm^{-1} results in the splitting observed in the spectra. The bottom panel of Figure 7 illustrates the spectra expected if no splitting occurred; each isotope would exhibit only two bands (I and II). The estimated wavenumbers for I and II differ by ~30 cm^{-1} for each isotope. The isotope shifts for I and II are in each case about 90% of calculated shift for an ideal diatomic oscillator. This schematic representation demonstrates that the observed spectrum for each isotope is grossly consistent with two major structures in which the bonding in the liganded O_2 differs markedly. Some spectral variations for the different isotopes are not well explained by this analysis. For example, bands not proposed to result from the 1125-cm^{-1} perturbation show somewhat different intensities. In particular, the highest frequency $^{16}O_2$ and $^{18}O_2$ band intensities differ, suggesting that other vibrational couplings may also be occurring (as observed for $^{18}O_2$ in model hemes; Bajdor et al., 1984). Nevertheless, the gross spectral patterns are adequately interpreted in terms of only two major O_2 vibrations.

Although the hemoglobins and myoglobins exhibit multiple dioxygen stretch bands, the oxygenated species of cytochrome *o* from *Vitreoscilla* was detected to have only one $^{16}O_2$ stretch band at 1134 cm^{-1} and only one $^{18}O_2$ stretch at 1078 cm^{-1} in the 1200–1030-cm^{-1} region (Choc et al., 1982). The $^{16}O_2$ to $^{18}O_2$ isotopic shift of 56 cm^{-1} is similar to that observed for the Hb and Mb spectra.

Comparison of O–O Stretch Bands in Spectra. Stretch bands for O_2 liganded to iron heme proteins with a proximal histidine have not been observed in Raman spectra (Bangchuroenpaurpong et al., 1986). However, they have been reported for cobalt-substituted heme proteins (Tsubaki & Yu, 1981; Mackin et al., 1983). Co-HbA exhibited Raman bands at 1152, 1137, and 1107 cm^{-1} for $^{16}O_2$ and at 1095 and 1063 cm^{-1} for $^{18}O_2$. A Co-Mb showed Raman bands at 1137 and 1103 cm^{-1} with a minor shoulder at 1153 cm^{-1} for $^{16}O_2$ and two $^{18}O_2$ bands at 1096 and 1069 cm^{-1}. The 1096-cm^{-1} band was very weak for Co-Mb. In contrast, the infrared spectra for Fe-Mbs reported here have clear bands at 1150 cm^{-1} for $^{16}O_2$ and 1090 cm^{-1} for $^{18}O_2$. Similar differences between infrared and Raman spectra are also found for the separated subunits of HbA. The $^{16}O_2$ Raman spectra for Co α-subunits

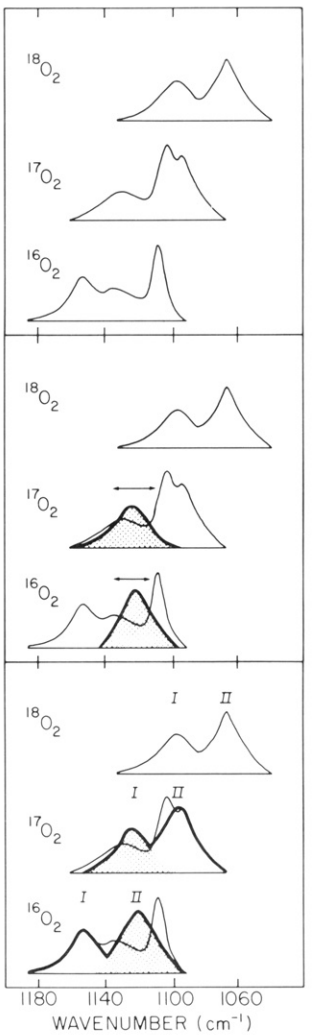

FIGURE 7: Schematic interpretation of dioxygen infrared spectra for hemoglobins and myoglobins liganded to $^{16}O_2$, $^{17}O_2$, and $^{18}O_2$. (Top) Typical $^{16}O_2$, $^{17}O_2$, and $^{18}O_2$ stretch bands as deduced from oxygen isotope difference spectra. The spectrum for each isotope contains multiple bands and an overall shape that is distinctly different from the spectra for the other isotopes. (Middle) A crosshatched band corresponding to the postulated unperturbed O–O stretch band for $^{16}O_2$ and $^{17}O_2$ at ~1125 cm^{-1} has been superimposed on the observed spectra of the top panel. The horizontal double-headed arrows indicate splitting of the unperturbed band to a strong lower frequency band and a weak higher frequency band. (Bottom) Postulated dioxygen stretch bands (I and II) that would be observed for each isotope if no perturbation from vibrational coupling occurred; these bands are represented by heavy lines for $^{17}O_2$ and $^{16}O_2$. For $^{18}O_2$ the observed spectrum is represented as equivalent to the unperturbed spectrum. For $^{17}O_2$, band I is split whereas for $^{16}O_2$ band II is split. Such an analysis supports two major bands (I and II) for each isotope separated by about 30 cm^{-1}. The magnitude of the isotope shifts is comparable to that for the shifts observed experimentally for model systems. The band shapes do not conform precisely to shapes predicted theoretically for single vibrations, which suggests additional minor bands are also present.

showed no strong 1155–1150-cm^{-1} band whereas β-subunits had a clear band in this region. Infrared spectra for the two naturally occurring Fe subunits showed similar intensities for all $^{16}O_2$ bands (Figure 5). Early infrared studies with HbA reconstituted with cobalt(II) deuteroporphyrin IX or iron(II) deuteroporphyrin IX showed O–O stretch bands for bound $^{16}O_2$ or $^{18}O_2$ that were similar for each metal (Maxwell & Caughey, 1974) and to those observed by Raman methods for HbA reconstituted with cobalt(II) protoporphyrin IX (Tsubaki & Yu, 1981; Mackin et al., 1983).

The resonance Raman studies of Co proteins also support an $\sim$1120-cm^{-1} perturbation that splits $^{16}O_2$ bands. However, in the Raman spectra the postulated splitting results in a lower frequency band near 1105 cm^{-1} that is much weaker than the higher frequency band near $\sim$1135 cm^{-1}. Since the infrared and Raman intensities are inversely related, the reciprocal intensity changes observed suggest that splitting results from a vibrational coupling that can be either in or out of phase. Such coupling could result in an intense transition dipole but enhanced polarizibility, at higher frequency. Since similar isotope-sensitive splitting patterns are observed in infrared and Raman spectra for both Fe- and Co-substituted porphyrins, band splitting that is due to Fermi resonance with a metal–oxygen overtone vibration is not expected (Nakamoto & Oshio, 1985). Splitting from such Fermi resonance was originally proposed to explain the two bands found in $HbAO_2$ at 1106 and 1155 cm^{-1} with the protein existing as a single structure, i.e., in only one conformation (Alben et al., 1978). However, the above analysis leads to the conclusion that there are two conformers (structures) with O_2 exhibiting two different structural forms at a single heme site.

Structural Implications. The energy and width of an O–O stretch band depends upon several factors: the bonding between iron and O_2, the steric requirements imposed by the dimensions of the ligand pocket, and the "solvent effects" of the immediate environment surrounding the bound O_2 in the pocket. Each of these factors can contribute to the 30-cm^{-1} difference between major conformers I and II. Bonding in metal ion–O_2 adducts exhibits an inverse relationship between O–O stretch band frequency and the electronegativity of the metal (Urban et al., 1982). For heme systems, iron electronegativity depends on the basicity of both the trans axial ligand (the proximal histidine in most hemoglobins and myoglobins) and the porphyrin nitrogens. The O–O stretch band frequency decreases as the trans axial ligand basicity increases (Kincaid et al., 1985). On the basis of model heme data, the highest O–O stretch frequency for $^{16}O_2$ in Hbs and Mbs at 1155–1150 cm^{-1} is consistent with a pK_a from 7 to 10 for the proximal histidine. In contrast, on this basis, the postulated lower frequency band near 1125 cm^{-1} would require an unreasonably large change in the proximal histidine basicity.

Considering possible solvent effects, the presumed H bonding from the distal histidine to dioxygen (Caughey, 1967; Phillips, 1984) may lower the O–O stretching frequency, but model studies suggest that it is unlikely that the entire 30-cm^{-1} difference in frequency between I and II can be due solely to H-bonding effects. In model heme systems the addition of solvents capable of H bonding (e.g., methanol) results in only minor red shifts ($\sim$5 cm^{-1}) (Bajdor et al., 1984; Kincaid et al., 1985). However, it is possible that larger red shifts due to H bonding can occur in the heme proteins due to a precise orientation of the distal histidine which enhances H-bonding effects. The spectra for Hb Zurich, whose β-subunits lack a distal histidine, is useful in evaluating H-bonding effects. Although the Hb Zurich $^{16}O_2$ spectrum exhibits two equal-intensity higher frequency bands at 1156 and 1151 cm^{-1} that can be attributed to differences in subunit structure, the lower frequency bands at 1130 and 1107 cm^{-1} are very similar to those found for HbA. The other approach to the evaluation of possible H bonding to dioxygen is a consideration of changes caused by the replacement of H_2O by D_2O on the O–O stretch band spectra. The effects of D_2O exchange on the spectra for sperm whale Mb are small (Figure 6). The major $^{16}O_2$ bands at 1148 and 1103 cm^{-1} were not detectably different in the two media, but minor changes in intensity were observed in the 1130–1120-cm^{-1} region. The most obvious difference occurs for the high-frequency $^{18}O_2$ band, where the exchange caused a shift to 1087 cm^{-1} from 1090 cm^{-1}. It should be noted that the angle of 88° between the O–O axis and the D bond observed by neutron diffraction (Phillips, 1980) places the deuterium where isotope substitution is expected to have a minimum effect on the O–O stretch frequency. Therefore, although some differences in H bonding to dioxygen may exist, the infrared evidence for H bonding is equivocal especially in regard to conformer II. Raman studies of cobalt-substituted $HbA^{16}O_2$ and $Mb^{16}O_2$ have been interpreted as evidence for H bonding to bound dioxygen (Kitagawa et al., 1982); the strong Raman stretch band near 1130 cm^{-1} is slightly blue-shifted upon replacement of H_2O by D_2O.

The 30-cm^{-1} difference in O–O stretch frequency between conformers may also be related to the orientations of the Fe–O–O and trans imidazole planes (Lavalette et al., 1984). In crystal structures of model hemes these orientations differ from those reported for heme proteins. The model oxy hemes consistently show a presumably sterically favorable arrangement, with the Fe–O–O plane bisecting Fe–pyrrole bonds and the axial imidazole positioned at an angle of 20–25° projected onto the N_1–Fe–N_3 heme axis (Jameson et al., 1980). In Hbs and Mbs the orientation of the proximal histidine is rigidly controlled by H bonding to the backbone carbonyl of the highly conserved F-4 leucine residue and the orientation of the bound dioxygen is modulated by its close contact with the distal histidine and the other well-conserved residues of the heme pocket, valine E-11 and phenylalanine CD-1 (Shaanan, 1983). The combined distal and proximal interactions apparently force a sterically unfavorable eclipsing orientation with the near superpositioning of the Fe–O–O plane and the plane of the axial histidine along the pyrrole N_1–Fe–N_3 heme axis. This sterically unfavorable geometry observed in diffraction studies is more prominent in Mb and α-subunits of HbA than in HbA β-subunits (Phillips, 1980; Shaanan, 1983); however, the large thermal parameters observed for the terminal atom of dioxygen suggests that the actual dioxygen structure is relatively mobile and may vary between the two limits of either eclipsing or bisecting. The computed single-crystal structures may therefore represent an average of the two structures represented by the two stretch bands (I and II) deduced here from O–O infrared spectra. Model oxy heme compounds generally show only O–O stretch bands similar to the higher frequency protein bands (Collman et al., 1976); therefore, the eclipsing of the Fe–O–O and imidazole planes may be responsible for the low-frequency protein conformer. The relative importance of the σ and π interactions of the axial ligands with iron will change as the orientation of plane of the proximal histidine with respect to the Fe–O–O plane is altered (Geiger et al., 1984; Scheidt & Chipman, 1986). In model oxy hemes the replacement of an axial imidazole by thiolate can decrease the O–O stretch frequency by 20 cm^{-1} (Nakamoto & Oshio, 1985). This large shift was attributed to enhanced π donation by the thiolate even though the difference in σ basicity of these

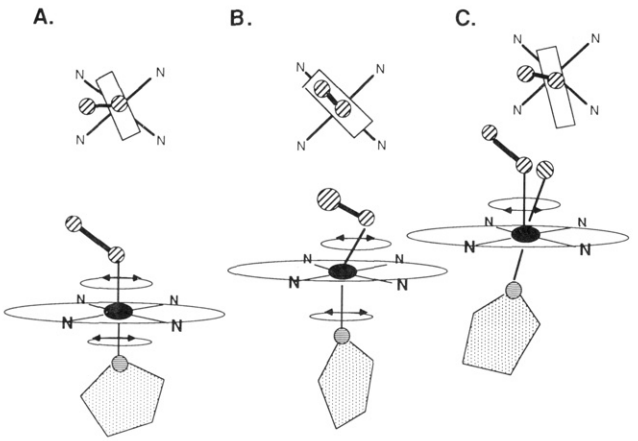

FIGURE 8: Schematic view of possible bonding geometries of O_2 and the imidazole of a proximal histidine in heme compounds. (A) The sterically favorable noneclipsed positions often observed in model oxy hemes. (B) The eclipsed positions observed in oxygenated Hb and Mb. (C) The off-axis distortion of the proximal histidine that occurs in axially strained compounds and upon deoxygenation of heme proteins. Two types of O_2 binding geometry are depicted in (A) bent-end-on and in (B) kinked. The qualitative difference between the two O_2 geometries is compared in (C). The double-headed arrows refer to angular rotations about the heme normal axis.

two ligands is not, by itself, large enough to cause such a large frequency shift. We suggest that the large red shift represented by the 1120-cm^{-1} $^{16}O_2$ conformer could result from a sterically unfavorable eclipsing orientation of the bound dioxygen and the plane of the axial proximal histidine, a structure that would enhance axial π interactions mediated through the metal.

The different types of bonding geometry considered above are shown schematically in Figure 8. The sterically favorable geometry observed in model oxy heme compounds is depicted in Figure 8A. A rotational alignment of the Fe–O–O and the proximal histidine planes corresponding to the time-averaged X-ray determined positions in heme proteins (Figure 8B) would necessitate close contact of the axial ligands with the heme pyrrole nitrogens but could be facilitated by favorable electronic interactions not only through the iron but by pyrrole nitrogens as well. A net increase in the extent of O–O bond reduction (corresponding to a lowered O–O stretch band frequency) could accompany these stereoelectronic changes in the Fe–O–O bonding geometry. Both geometries (Figure 8A,B) will have rotational freedom that is sensitive to the protein structure at both the distal and proximal heme sites. A third structural variation depicted in Figure 8C involves displacement of the proximal histidine off the heme normal axis. In this type of structural deformation the rotational freedom of the proximal histidine is restricted and favorable electronic interactions that could facilitate the alignment of the Fe–O–O plane over a pyrrole nitrogen may be lost. Alteration in the relative orientation of the Fe–O–O plane with respect to the proximal imidazole not only correlates well with the differences observed in O–O stretch frequency but also suggests a mechanism for control of O_2 affinity that would couple both distal and proximal effects. Such a mechanism could be more effective and sensitive than is possible with the commonly proposed mechanism involving only the out-of-plane and off-axis movement of the proximal histidine upon deoxygenation.

Two O–O stretch bands have also been seen in the infrared spectra of model hemes with no backside axial ligand (Watanabe et al., 1984). The higher frequency band found from 1195 to 1190 cm^{-1} (depending on the porphyrin and the solvent) has been ascribed to end-on-bound dioxygen. The high frequency of this band presumably reflects a reduced electronegativity of iron(II) as a result of the lack of an axial base trans to O_2. A less intense second band is found near 1105 cm^{-1} and has been suggested to result from a side-on-bonded dioxygen. A band with similar frequency is also observed in the Hbs and Mbs, but the intensities relative to the higher frequency band(s) are much greater in the proteins. For the model hemes the higher frequency band is about 6-fold more intense than the 1105-cm^{-1} band, which is consistent with the lower intensity that is expected for a symmetric side-on-bonded species that has a smaller net transition dipole. Furthermore, since the intense band found near 1105 cm^{-1} in hemoglobins and myoglobins appears to result from the splitting of a vibration that would be near 1125–1120 cm^{-1} if unperturbed, neither the intensity nor the frequency of the lower heme protein band provides convincing evidence for a side-on bound dioxygen. Nevertheless, there is a basis for suggesting that significant variations in the bonding interactions between the trans axial proximal histidine and iron in hemoglobins can occur. In nitrosyl-HbA a weakening of the bonding between the proximal histidine and iron(II) upon addition of inositol hexakis(phosphate) is indicated in NO infrared, optical, and electron paramagnetic resonance spectra (Maxwell & Caughey, 1976; Perutz et al., 1976). The definitive infrared evidence for a large difference in O–O bond order for the two dioxygen conformers undoubtedly reflects some structural differences that involve both distal and proximal histidines. More detailed insight into the nature of these structural differences must await a better understanding of the effects of structure and environment on O–O stretch bands.

Registry No. $HbAO_2$, 9062-91-3; $HbZhO_2$, 59029-76-4; O_2, 7782-44-7; ^{17}O, 13968-48-4; ^{18}O, 14797-71-8.

REFERENCES

Alben, J. O., Bare, G. H., & Moh, P. P. (1978) in *Biochemical and Clinical Aspects of Hemoglobin Abnormalities* (Caughey, W. S., Ed.) p 607, Academic, New York.

Antonini, E., & Brunori, M. (1971) in *Hemoglobin and Myoglobin in Their Reactions with Ligands* (Neuberger, A., Ed.) p 1, North-Holland, New York.

Bajdor, K., Kincaid, J. R., & Nakamoto, K. (1984) *J. Am. Chem. Soc. 106*, 7741.

Bangcharoenpaurpong, O., Rizos, A. K., Champion, P. M., Jollie, D., & Sligar, S. G. (1986) *J. Biol. Chem. 261*, 8089.

Barlow, C. H., Maxwell, J. C., Wallace, W. J., & Caughey, W. S. (1973) *Biochem. Biophys. Res. Commun. 55*, 91.

Brozozowski, A., Derewenda, Z., Dodson, E., Grabowski, M., Liddington, R., Skarzynski, T., & Vallely, D. (1984) *Nature (London) 307*, 74.

Bucci, E. (1981) *Methods Enzymol. 76*, 97.

Bunn, H. F., & Forget, B. G. (1986) in *Hemoglobin: Molecular, Genetic and Clinical Aspects* (Dyson, J., Ed.) p 1, Saunders, Philadelphia.

Caughey, W. S. (1967) *Annu. Rev. Biochem. 36*, 611.

Caughey, W. S. (1980) in *Methods for Determining Metal Ion Environments in Proteins: Structure and Function of Metalloproteins* (Darnall, D. W., & Wilkins, R. G., Eds.) p 95, Elsevier/North-Holland, New York.

Caughey, W. S., & Watkins, J. A. (1985) in *Handbook of Methods for Oxyradical Research* (Greenwald, R., Ed.) p 95, CRC Press, Boca Raton, FL.

Caughey, W. S., Barlow, C. H., Maxwell, J. C., Volpe, J. A., & Wallace, W. J. (1975) *Ann. N.Y. Acad. Sci. 244*, 1.

Caughey, W. S., Choc, M. G., & Houtchens, R. A. (1979) in *Biochemical and Clinical Aspects of Oxygen* (Caughey,

W. S., Ed.) p 1, Academic, New York.
Caughey, W. S., Shimada, H., Choc, M. G., & Tucker, M. P. (1981) *Proc. Natl. Acad. Sci. U.S.A. 78*, 2903.
Caughey, W. S., Shimada, H., Tucker, M. P., Kawanishi, S., Yoshikawa, S., & Young, L. J. (1982) in *Oxygenases and Oxygen Metabolism* (Nazaki, M., Yamamoto, S., Ishimura, Y., Coon, M. J., Ernster, L., & Estrabrook, R. W., Eds.) p 429, Academic, New York.
Caughey, W. S., Shimada, H., Hazzard, J. H., Houtchens, R. A., Potter, W. T., & Einarsdottir, O. (1983) *Fed. Proc., Fed. Am. Soc. Exp. Biol. 42*, 2000.
Choc, M. G., & Caughey, W. S. (1981) *J. Biol. Chem. 256*, 1831.
Choc, M. G., Webster, D. A., & Caughey, W. S. (1982) *J. Biol. Chem. 257*, 865.
Collman, J. P., Brauman, J. I., Halbert, T. R., & Suslick, K. S. (1976) *Proc. Natl. Acad. Sci. U.S.A. 73*, 3333.
Dozy, A. M., Kleihauer, E. F., & Huisman, T. H. (1968) *J. Chromatogr. 32*, 723.
Geiger, D. K., Lee, Y. J., & Scheidt, W. R. (1984) *J. Am. Chem. Soc. 106*, 6339.
Gotoh, T., & Shikama, K. (1974) *Arch. Biochem. Biophys. 163*, 476.
Himmel, M. E., & Squire, P. G. (1981a) *Int. J. Pept. Protein Res. 17*, 365.
Himmel, M. E., & Squire, P. G. (1981b) *J. Chromatogr. 210*, 443.
Jameson, G. B., Molinaro, F. S., Ibers, J. A., Collman, J. P., Brauman, J. I., Rose, E., & Suslick, K. S. (1980) *J. Am. Chem. Soc. 102*, 3224.
Jelkmann, W., & Bauer, C. (1976) *Anal. Biochem. 75*, 382.
Kawanishi, S., & Caughey, W. S. (1985) *J. Biol. Chem. 260*, 4622.
Kincaid, J. R., Proniewicz, L. M., Bajdor, K., Bruha, A., & Nakamoto, K. (1985) *J. Am. Chem. Soc. 107*, 6775.
Kitagawa, T., Ondrias, M. R., Rousseau, D. L., Ikeda-Saito, M., & Yonetani, T. (1982) *Nature (London) 298*, 869.
Lavalette, D., Tetreau, C., Mispelter, J., Momenteau, M., & Lhoste, J.-M. (1984) *Eur. J. Biochem. 145*, 555.
Mackin, H. C., Tsubaki, M., & Yu, Y.-T. (1983) *Biophys. J. 41*, 349.
Maxwell, J. C., & Caughey, W. S. (1974) *Biochem. Biophys. Res. Commun. 60*, 1309.
Maxwell, J. C., & Caughey, W. S. (1976) *Biochemistry 15*, 388.
Maxwell, J. C., & Caughey, W. S. (1978) *Methods Enzymol. 54*, 302.
Maxwell, J. C., Volpe, J. A., Barlow, C. H., & Caughey, W. S. (1974) *Biochem. Biophys. Res. Commun. 58*, 166.
McCoy, S., & Caughey, W. S. (1970) *Biochemistry 9*, 2387.
Nakamoto, K., & Oshio, H. (1985) *J. Am. Chem. Soc. 107*, 6518.
Orii, Y., & Washio, N. (1977) *J. Biochem. (Tokyo) 81*, 495.
Perutz, M. F., Kilmartin, J. V., Nagai, K., Szabo, A., & Simon, S. R. (1976) *Biochemistry 15*, 378.
Phillips, S. E. V. (1980) *J. Mol. Biol. 142*, 531.
Phillips, S. E. V., & Schoenborn, B. P. (1981) *Nature (London) 292*, 81.
Riggs, A. (1981) *Methods Enzymol. 76*, 5.
Rothgeb, T. M., & Gurd, F. R. N. (1978) *Methods Enzymol. 52*, 473.
Scheidt, W. R., & Chipman, D. M. (1986) *J. Am. Chem. Soc. 108*, 1163.
Shaanan, B. (1982) *Nature (London) 296*, 683.
Shaanan, B. (1983) *J. Mol. Biol. 171*, 31.
Shimada, H., & Caughey, W. S. (1982) *J. Biol. Chem. 257*, 11893.
Tsubaki, M., & Yu, N.-T. (1981) *Proc. Natl. Acad. Sci. U.S.A. 78*, 3581.
Uchida, K., Bandow, H., Makino, R., Sakaguchi, K., Iizuka, T., & Ishimura, Y. (1985) *J. Biol. Chem. 260*, 1400.
Urban, M. W., Nonaka, Y., & Nakamoto, K. (1982) *Inorg. Chem. 21*, 1046.
Wallace, W. J., Houtchens, R. A., Maxwell, J. C., & Caughey, W. S. (1982) *J. Biol. Chem. 257*, 4966.
Watanabe, T., Ama, T., & Nakamoto, K. (1984) *J. Phys. Chem. 88*, 440.
Winterbourn, C. C. (1985) *EHP, Environ. Health Perspect. 64*, 321.
Yamazaki, I., Yokota, K.-N., & Shikama, K. (1964) *J. Biol. Chem. 239*, 4151.
Yip, Y. K., Waks, M., & Beychok, S. (1977) *Proc. Natl. Acad. Sci. U.S.A. 74*, 64.
Yoshikawa, S., O'Keeffe, D., & Caughey, W. S. (1985) *J. Biol. Chem. 260*, 3518.
Yu, N.-T. (1986) *Methods Enzymol. 130*, 350.